14. Tetsuji, O., Ernst, O. P., Krzysztof, P. et al., Activation of rhodopsin: new insights from structural and biochemical studies, Trends Biochem. Sci., 2001, 26: 318—324.
15. Horn, F., Vriend, G., Cohen, F. E., Collecting and harvesting biological data: the GPCRDB and NuleaRDB information systems, Nucleic Acids Res., 2001, 29: 346—349.
16. Dixon, R. A. F., Kobilka, B. K., Strader, D. J. et al., Cloning the gene and cDNA for mammalian β2-adrenergic receptor and homology with rhodopsin, Nature, 1986, 321: 75—79.
17. Horn, F., Weare, J., Beukers, M. W. et al., GPCRDB: an information system for G protein-coupled receptors, Nucleic Acids Res., 1998, 26: 275—279.
18. Beukers, M. W., Kristiansen, K., Ijzerman, A. P. et al., TinyGRAP database: a bioinformatics tool to mine G-protein-coupled receptor mutant data, Trends Pharmacol. Sci., 1999, 20: 475—477.
19. Alexey, G. M., Steven, E. B., Tim, H. et al., SCOP: A structural classification of protein database for the investigation of sequences and structures, J. Mol. Biol., 1995, 247: 536—540.
20. Lee, D. K., George, S. R., Evans, J. F. et al., Orphan G protein-coupled receptors in the CNS, Curr. Opin. Pharmacol., 2001, 1: 31—39.
21. Howard, D. A., McAllister, G., Feighner, S. D. et al., Orphan G-protein-coupled receptors and natural ligand discovery, Trends Pharmacol. Sci., 2001, 22: 132—140.
22. Venter, J. C., Adams, M. D., Myers, E. W. et al., The sequence of the human genome, Science, 2001, 291: 1304—1351.
23. Civelli, O., Nothacker, H. P., Saito, Y. et al., Novel neurotransmitters as a natural ligands of orphan G-protein-coupled receptors, Trends Neurosci., 2001, 24: 230—237.
24. Lee, D. K., Nguyen, T., Lynch, K. R. et al., Discovery and mapping of ten novel G protein-coupled receptor genes, Gene, 2001, 275: 83—91.
25. Lee, D. K., George, S. R., Cheng, R. et al., Identification of four novel human G protein-coupled receptors expressed in the brain, Mol. Brain Res., 2001, 86: 13—22.
26. Wittenberger, T., Schaller, H. C., Hellebrand, S., An expressed sequence tag data mining strategy succeeding in the discovery of new G-protein-coupled receptors, J. Mol. Biol., 2001, 307: 799—813.
27. Krogh, A., Larsson, B., Heijne, G. V. et al., Predicting transmembrane protein topology with a hidden markov model: application to complete genomes, J. Mol. Biol., 2001, 305: 567—580.
28. Dong, X., Han, S. K., Zylka, M. J. et al., A diverse family of GPCRs expressed in specific subsets of nociceptive sensory neurons, Cell, 2001, 106: 619—632.
29. Borowsky, B., Adham, N., Jones, K. A. et al., Trace amines: Identification of a family of mammalian G protein-coupled receptors, PNAS, 2001, 98: 8966—8971.
30. Altschul, S. F., Gish, W., Miller, W. et al., Basic local alignment search tool, J. Mol. Biol., 1990, 215: 403—410.
31. Falquet, L., Pagni, M., Bucher, P. et al., The PROSITE database, its status in 2002, Nucleic Acids Res., 2002, 30: 235—238.
32. Altschul, S. F., Madden, T. L., Schäffer, A. A. et al., Gapped BLAST and PSI-BLAST: a new generation of protein database search programs, Nucleic Acids Res., 1997, 25: 3389—3402.

(Received September 8, 2002; accepted December 6, 2002)

Chinese Science Bulletin 2003 Vol. 48 No. 6 516—518

Room-temperature ferromagnetic semiconductor $Mn_xGa_{1-x}Sb$

CHEN Nuofu[1,2], ZHANG Fuqiang[1,2], YANG Junling[1,2], LIU Zhikai[1], YANG Shaoyan[1], CHAI Chunlin[1], WANG Zhanguo[1], HU Wenrui[2] & LIN Lanying[1,2]

1. Key Laboratory of Semiconductor Materials Science, Institute of Semiconductors, Chinese Academy of Sciences, Beijing 100083, China;
2. National Microgravity Laboratory, Chinese Academy of Sciences, Institute of Mechanics, Beijing 100080, China

Correspondence should be addressed to Chen Nuofu (e-mail: nfchen@red.semi.ac.cn)

Abstract **Ferromagnetic semiconductor $Mn_xGa_{1-x}Sb$ single crystals were fabricated by Mn-ions implantation, deposition, and the post annealing. Magnetic hysteresis-loops in the $Mn_xGa_{1-x}Sb$ single crystals were obtained at room temperature (300 K). The structure of the ferromagnetic semiconductor $Mn_xGa_{1-x}Sb$ single crystal was analyzed by X-ray diffraction. The distribution of carrier concentrations in $Mn_xGa_{1-x}Sb$ was investigated by electrochemical capacitance-voltage profiler. The content of Mn in $Mn_xGa_{1-x}Sb$ varied gradually from $x = 0.09$ near the surface to $x = 0$ in the wafer inner analyzed by X-ray diffraction. Electrochemical capacitance-voltage profiler reveals that the concentration of p-type carriers in $Mn_xGa_{1-x}Sb$ is as high as 1×10^{21} cm^{-3}, indicating that most of the Mn atoms in $Mn_xGa_{1-x}Sb$ take the site of Ga, and play a role of acceptors.**

Keywords: $Mn_xGa_{1-x}Sb$, ferromagnetic semiconductor, diluted magnetic semiconductors.

Magnetic semiconductors can combine the semiconducting properties with magnetic properties, and be used in these applications, such as magnetic field sensors, magnetic memory elements and, in long range, quantum computation and communication. Ⅱ-Ⅵ based diluted magnetic semiconductors (DMSs) have been extensively studied[1—3], because some magnetic ions are easily incorporated into Ⅱ-Ⅵ compounds by substituting group Ⅱ atoms. It was conventionally considered that the equilibrium solubility of magnetic ions in Ⅲ-Ⅴ compounds is quite low (~10^{19} cm^{-3}). In fact, the content x in $Mn_xGa_{1-x}Sb$ can be as high as 15%[4,5]. The difficulty in growing Ⅲ-Ⅴ based DMS epitaxy-layers is due to the mismatch of lattice constants between Ⅲ-Ⅴ based DMS and its substrate. Compared with Ⅱ-Ⅵ based DMSs, Ⅲ-Ⅴ based DMSs possess greater advantages, because doping control is far more difficult in Ⅱ-Ⅵ than in Ⅲ-Ⅴ compounds. Up to now, the highest Curie temperature in Ⅲ-Ⅴ based DMSs is about 110 K, i.e. for $Ga_{0.95}Mn_{0.05}As$[6,7], realized by molecular beam epitaxy

(MBE) at low temperature (~200℃)[8—10].

In this report, zinc-blende ferromagnetic semiconductor $Mn_xGa_{1-x}Sb$ single crystals were prepared by Mn-ions implantation, deposition, and the post annealing. Magnetic hysteresis-loops in the $Mn_xGa_{1-x}Sb$ single crystals were obtained at room temperature (300 K). The structure and Mn content in zinc-blende ferromagnetic semiconductor $Mn_xGa_{1-x}Sb$ single crystal were analyzed by X-ray diffraction. The distribution of carrier concentrations in $Mn_xGa_{1-x}Sb$ was investigated by electrochemical capacitance-voltage profiler (ECC-V).

The zinc-blende $Mn_xGa_{1-x}Sb$ single crystals were prepared by a low-energy ion-beam deposition (LEIBD) system. There are magnetic analyzers in the LEIBD system, with which the manganese can be purified as pure as isotope. First, the manganese ions with energy of 1 keV were implanted into unintentionally doped p-type (001) oriented GaSb wafer in the depth of about 70 nm at 200℃. Then, the manganese ions with energy of 100 eV were deposited on the surface of the wafer, which formed a thin layer about 5 nm thick. After the Mn-ions implantation and deposition, the wafers were annealed at 400 °C in an argon ambience for 30 min. The thin layer of manganese on the surface of the GaSb wafer can prevent the implanted manganese ions from diffusing out of the surface of the wafer, and can keep the content of Mn at a high level near the surface of $Mn_xGa_{1-x}Sb$ while annealing.

The magnetic properties of the $Mn_xGa_{1-x}Sb$ samples were studied using vibrating sample magnetometer (VSM) LDJ9600, and the measurements were carried out at room temperature (300 K). Fig. 1 shows a typical hysteresis-loop measured by VSM from a $Mn_xGa_{1-x}Sb$ sample. The detailed results of the measurements were shown in Table 1. The highest saturation magnetization and residual magnetization are 9.331×10^{-4} and 3.035×10^{-4} e.m.u., respectively. The largest coercive force in these samples is 14916.63 A • m^{-1}. These results confirm that these $Mn_xGa_{1-x}Sb$ samples are ferromagnetic at room temperature. It can also be seen in Fig. 1 that the absolute value of

Table 1 Magnetic properties measured by vibrating sample magnetometer

Sample number	Saturation magnetization (e.m.u)	Residual magnetization (e.m.u)	Coercive force /A • m^{-1}
1012	4.201×10^{-4}	1.117×10^{-4}	6379.051
1024	9.331×10^{-4}	2.872×10^{-4}	11176.51
1026	3.517×10^{-4}	6.804×10^{-5}	13606.23
1028	8.549×10^{-4}	3.035×10^{-4}	9611.628
1036	3.078×10^{-4}	9.218×10^{-5}	14916.63

magnetization decreases after the magnetic field surpasses the saturation value. The reason for this is that the GaSb substrate is diamagnetic, and after the saturated magnetization the diamagnetic moment in GaSb becomes obvious.

X-ray diffraction was utilized to investigate the structure and contents of the samples. Two diffraction modes, i.e. q-$2q$ and the small angle of incidence were used in the investigation. No new diffraction peak was found in these X-ray diffraction measurements except those diffracted from GaSb. A typical q-$2q$ diffraction curve (solid line) from a $Mn_xGa_{1-x}Sb$ sample near (002) reflection is shown in Fig. 2. Compared with the diffraction curve from a GaSb wafer (dotted line) in the same figure, the left site of the diffraction curve, from A to B, is obviously bulging. The implantation of Mn-ions and their diffusion in the GaSb wafer are responsible for this bulge of the diffraction curve. The Mn-ions take the sites of Ga in GaSb and make the lattice expand. Because the Mn-ions diffused into the GaSb continuously, the content of Mn gradually decreases with the increase of depth, and so does the lattice expanse. Point A in Fig. 2 is corresponding to the maximum lattice expanse in $Mn_xGa_{1-x}Sb$. According to a model dealing with the substitutes in zinc-blende crystal[11] and its modification[12], the maximum content of Mn in $Mn_xGa_{1-x}Sb$ resulting in the maximum lattice expanse can be calculated as $x = 0.09$. Therefore, the content of Mn gradually decreases from $x = 0.09$ near the surface to $x = 0$ in the $Mn_xGa_{1-x}Sb$ wafer inner. The lattice strain also gradually decreases from

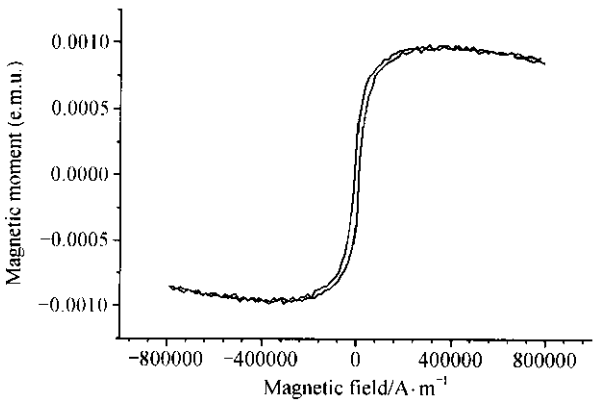

Fig. 1. Magnetic hysteresis-loop measured by vibrating sample magnetometer from a $Mn_xGa_{1-x}Sb$ sample.

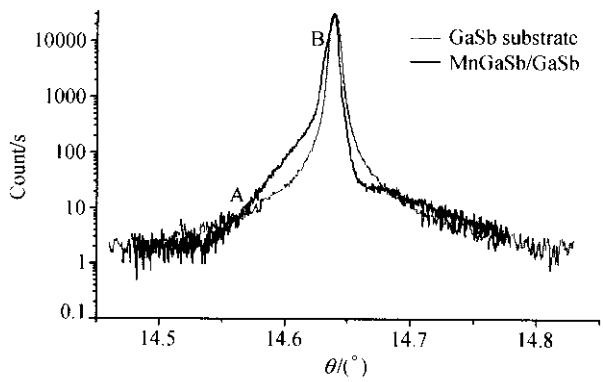

Fig. 2. X-ray diffraction curves from $Mn_xGa_{1-x}Sb$/GaSb (solid line) and GaSb (dotted line) near (002) reflection.

$\Delta a/a_0$ = 0.005 near the surface to $\Delta a/a_0$ = 0 in the $Mn_xGa_{1-x}Sb$ wafer inner. This gradual change in lattice constant enables $Mn_xGa_{1-x}Sb$ to keep its zinc-blende structure stable.

On the other hand, if Mn atoms take the sites of Ga in GaSb, the antisites Mn_{Ga} will play a role of acceptors. For making it clear, the concentration profile of carriers in $Mn_xGa_{1-x}Sb$/GaSb was measured by ECC-V technique. The typical depth profile of carrier concentrations in $Mn_xGa_{1-x}Sb$/GaSb is shown in Fig. 3. The carrier concentration near the surface of the sample is about 1×10^{21} cm^{-3}, and it drops abruptly to 1×10^{19} cm^{-3} within a depth of 70 nm. The drop in carrier concentrations resulted from the Mn-ion implantation and the diffusion of Mn atoms during the annealing. Then the carrier concentration drops flatly to about 9×10^{17} cm^{-3} in the depth of 4 μm. The major carriers in $Mn_xGa_{1-x}Sb$ are holes, which indicates that the Mn atoms play a role of acceptors in $Mn_xGa_{1-x}Sb$.

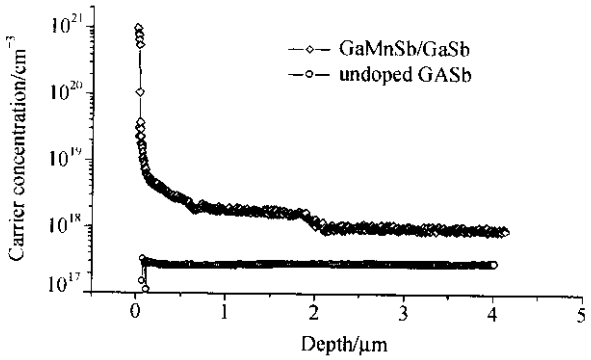

Fig. 3. Depth profile of carrier concentrations in $Mn_xGa_{1-x}Sb$/GaSb (upper) and in unintentionally dope GaSb (lower).

For comparison, the carrier concentration profile in unintentionally doped p-type GaSb wafer was also measured with ECC-V (Fig. 3). The concentration of carriers is about 2.9×10^{17} cm^{-3}, and distributes uniformly.

The density of atoms in GaSb is 1.78×10^{22} cm^{-3}, and the highest concentration of carries in $Mn_xGa_{1-x}Sb$ is about 1×10^{21} cm^{-3}. So the ratio of the highest carrier concentration to the density of atoms is 5.6%, or x = 0.10 in $Mn_xGa_{1-x}Sb$. This result is consistent with X-ray analyses, and indicates that most of the Mn atoms in $Mn_xGa_{1-x}Sb$ take the sites of Ga in GaSb.

In summary, room-temperature ferromagnetic semiconductor $Mn_xGa_{1-x}Sb$ single crystals have been prepared by implanting Mn-ions into GaSb wafers exploiting a lowenergy ion-beam deposition system, and the post annealing. Magnetic hysteresis-loops were obtained from the $Mn_xGa_{1-x}Sb$ samples at room temperature. X-ray diffraction analyses show that the $Mn_xGa_{1-x}Sb$ samples are thermally stable zinc-blend structure, and the content of Mn gradually decreases from x = 0.09 near the surface to x = 0 in the $Mn_xGa_{1-x}Sb$ wafer inner. Electrochemistry capacitance-voltage profiler reveals that the concentration of p-type carriers in $Mn_xGa_{1-x}Sb$ is as high as 1×10^{21} cm^{-3}, indicating that most of the Mn atoms in $Mn_xGa_{1-x}Sb$ take the sites of Ga, and play a role of acceptors.

Acknowledgements The authors would like to thank J. L. Wu, C. T. Peng, X. L. Zhang, X. R. Zhong, M. C. Zhang and X. Q. Bao for their helps to this work. The work was jointly supported by the National Natural Science Foundation of China (Grant No. 60176001) and Special Funds for the Major State Basic Research Projects (Grant Nos. G20000365 and G20000683).

References

1. Mac, W., Heribich, M., Nguyen, T. K. et al., The s-d and p-d exchange interaction in $Zn_{1-x}Fe_xTe$, Phys. Rev., 1996, B53(15): 9532—9535.
2. Meiman, D., Petrou, A., Bloom, S. H. et al., Nonmagnetic ground state of Fe^{2+} in CdSe: Absence of bound magnetic polaron, Phys. Rev. Lett., 1988, 60(18): 1876—1879.
3. Haury, A., Wasiela, A., Arnoult, A. et al., Observation of a ferromagnetic transition induced by two-dimensional hole gas in modulation-doped CdMnTe quantum wells, Phys. Rev. Lett., 1997, 79(3): 511—514.
4. Hand Book of Ternary Alloy Diagram (in CD version), ASM International, 1995.
5. Szatkowski, J., Placzek-Popko, E., Hajdusianek, A. et al., Deep electron states in gallium-doped CdMnTe mixed crystals, J. Cryst. Growth, 1996, 161/162: 282—285.
6. Kacman, P., Spin interactions in diluted magnetic semiconductors and magnetic semiconductor structures, Semicond. Sci. Technol., 2001, 16(4): R25—R39.
7. Matsukura, F., Ohno, H., Shen, A., Transport properties and origin of ferromagnetism in (Ga, Mn)As, Phys. Rev., 1998, B57(4): R2037—R2040.
8. Hayashi, T., Tanaka, M., Nishinaga, T. et al., Magnetic and magnetotransport properties of new III-V diluted magnetic semiconductors: GaMnAs, J. Appl. Phys., 1997, 81(8): 4865—4867.
9. Ohno, H., Munekata, H., Molnar, S. et al., New III-V diluted magnetic semiconductors, J. Appl. Phys., 1991, 69(8): 6103—6108.
10. Karar, N., Basu, S., Venkatarghavan, R. et al., Absorption and photoluminescence spectra of the diluted magnetic semiconductor $Ga_{1-x}Fe_xSb$, J. Appl. Phys., 2000, 88(2): 924—926.
11. Chen, N. F., Wang, Y. T., He, H. J. et al., Effects of point defects on lattice parameters of semiconductors, Phys. Rev., 1996, B54(12): 8516—8521.
12. Chen, N. F., Xiu, H. X., Yang, J. L. et al., Content analyses in GaMnAs by double-crystal X-ray diffraction, Chinese Science Bulletin, 2002, 47(4): 274—275.

(Received October 16, 2002)